Chromatic adaptation model for the early visual system

Chihiro Imai† and Hideyuki Suzuki†‡

† Graduate School of Information Science and Technology, University of Tokyo
4-6-1 Komaba, Meguro-ku, Tokyo 153-8505, Japan
‡ Institute of Industrial Science, University of Tokyo
4-6-1 Komaba, Meguro-ku, Tokyo 153-8505, Japan
Email: chihi@sat.t.u-tokyo.ac.jp, hideyuki@iis.u-tokyo.ac.jp

We propose a computational model of the primate visual pathway, which explains the change in color appearance during and after the adaptation with a broad range of temporal scales. The model assumes that the neuronal plasticity plays a key role in the long-term adaptations. Our model reproduces the dynamic properties of color vision reported in the previous experimental studies. Additionally, we applied the current model to various conditions of chromatic illumination, providing testable predictions on the color appearances and their dynamics in changing environments.

1. Introduction

Light that reaches the retina changes in various time scales ranging from tens of milliseconds to several decades as senescent changes in ocular media density. The intensity varies in more than 10 log units. Nevertheless, our vision achieves to maintain a stable color perception. The visual system makes adaptive adjustments to maintain optimal response over a wide range of ambient light levels and chromaticity.

One of the functions that mediate color appearance is chromatic adaptation. Chromatic adaptation is defined as sensitivity regulation of color vision. Psychophysical experiments reported that chromatic adaptation can occur at different stages in the visual pathway from the retina to the cortical higher cognitive levels and can have different temporal scales (Hughes & DeMarco, 2003).

Adaptation period influences the temporal characteristics of color perception induced by chromatic adaptation. Chromatic adaptation within several tens of seconds can induce afterimage and short-term shift of equilibrium color. Although the equilibrium yellow, the color perceived as neither reddish nor greenish, is profoundly changed by short-term adaptations, it returns to the normal perception immediately after the release from adaptation (Eisner & Enoch, 1982). In contrast, recent studies report that long-term adaptations continuing for weeks shift the yellow perception progressively away from the normal, and the changed perceptions persist for weeks in the absence of exposure to chromatic alteration (Neitz et al., 2002; Belmore & Shevell, 2008).

Existing computational studies are not enough to provide a unified model which accounts for both the brief and the sustained shifts in chromatic perception led by short- and long-term adaptations, respectively. Little studies focus on the dynamics and the plasticity of the visual system during chromatic adaptation in various time scales. In this study, we propose a computational model of the primate visual pathway, which explains the change in color appearance during and after the adaptation with a broad range of temporal scales. The model assumes that the neuronal plasticity plays a key role in the long-term adaptation.

2. Model

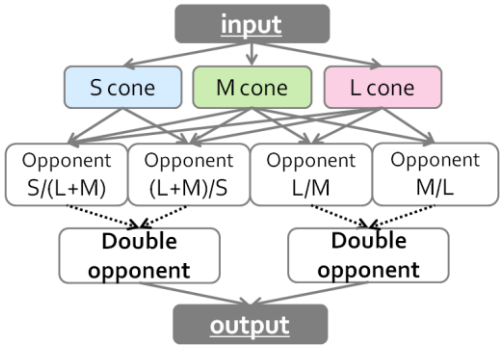

Fig.1 Schematic diagram of the proposed model (ON-pathway only). The model assumes long-term synaptic plasticity between opponent cells and double opponent cells, shown in dotted line in the figure.

We proposes a model which consists of three layers; cones, opponent cells, and double opponent cells. The model considers both ON- and OFF-pathway. The schematic diagram of ON pathway is presented in Fig.1. We consider adaptation in all stages, and long-term synaptic plasticity at the connection between opponent cells and double opponent cells, based on retinal and cortical mechanisms of adaptation.

2.1. Cones

The first stage describes the retinal color-coding channels; L, M, and S cones which are sensitive to long, middle, and short wavelength, respectively, assuming photopic vision. The input is given as the spectrum distribution I(λ) (Eq. 1), where $p_{L,M,S}(\lambda)$ represents the

spectral sensitivity of each cone type (Smith and Pokorny, 1975). r stands for responses of L, M and S.

$$r(t = \int p_{L,M,S}(\lambda) I(t,\lambda) d\lambda \cdot \quad (1)$$

Each cone response after adaptation r^* depends on both the strength and the adaptation duration of the input. Adaptation in the cones is modeled as follows:

$$r^*(t) = \frac{r(t)^n}{R(t)^n + \sigma(r,t)^n}, \quad (2)$$

$$\sigma(r,t) = \alpha R_b(t) + \beta, \quad (3)$$

$$R_b(t) = r(t) * f_b(t), \quad (4)$$

$$f_b(t) = \frac{1}{\tau_b} \exp(-t/\tau_b), \quad (5)$$

$$\tau_b = \frac{\tau_n}{1 + |r(t) - R_b(t)| / R_n}, \quad (6)$$

where n, α, β, τ_n, and R_n are constant, we follow the study by Dahari & Spitzer, 1996. A convolution of $R_b(t)$ with the dynamic temporal filter $f_b(t)$ is carried out in Eq. (4).

2.2. Input to opponent cells

Opponent cells have concentric center-surround receptive field structure and respond oppositely to signal in the center and surround of their receptive fields. The spatial response property of two sub-regions is expressed with difference-of-Gaussians. Before adaptation, the responses r (x, y, t) which are located at (x, y) is expressed as follows:

$$f_{cen,sur}(x,y) = \frac{\exp[-(x^2 + y^2)/q_{cen,sur}{}^2]}{\pi q_{cen,sur}{}^2}, \quad (7)$$

$$r_{cen,sur}(x,y,t) = \iint r(x,y,t) f_{cen,sur}(x,y) dxdy, \quad (8)$$

where the constant $q_{cen,sur}$ is the radius of the receptive field. The diameter of the annular surround is three times larger than that of the center region.

The model considers both ON- and OFF-pathway. Therefore, there are eight types of opponent cells; ON-center L, OFF-center L, ON-center M, OFF-center M, ON-center S, OFF-center S, ON-center (L+M), and OFF-center (L+M). Center region of ON-center cell receives excitatory signal from the corresponding cone, and surround receives inhibitory signal, respectively. On the other hand, center region of OFF-center cell receives inhibitory signal, and surround receives excitatory signal.

$$R_{L(+)/M(-)} = r^*_{L\_cen} - r^*_{M\_sur}, \quad (9)$$

$$R_{S(+)/(L+M(-))} = r^*_{S\_cen} - r^*_{(L+M)\_sur}, \quad (10)$$

$$R^*_{(L+M)} = \frac{r_L{}^* + r_M{}^*}{2}, \quad (11)$$

where the suffixes represent both the cone type and the sub-region from which the opponent cell receive the signal. The responses of opponent cells R^*_{L+M} is calculated by the average of the response of L cone and M cone (Eq. 11).

The temporal characteristics of ON- and OFF-center cells are different, since the time constants of excitatory synapse are smaller than that of inhibitory synapse (Eqs.15, 16, 18, and 20). Opponent cells are distributed from the layer of the retinal ganglion cell to the cortex.

2.3. Input to double opponent cell

Double opponent cells also have center-surround receptive field structure. However, both center and surround sub-regions of double opponent cells show color opponency. Double opponent cells are clustered within localized regions of V1 called blobs. The responses subtracted off-center opponent cells from on-center opponent cell are used as the inputs of double opponent cells, which receive the input from the same cones. The signal from the corresponding opponent cells is expressed with the Eqs. (12) and (13):

$$R_{L+M-/L-M+} = R^*_{L(+)/M(-)} - R^*_{L(-)/M(+)}, \quad (12)$$

$$R_{S+(L+M)-/S-(L+M)+} = R^*_{S(+)/(L+M)(-)} - R^*_{S(-)/(L+M)(+)}, \quad (13)$$

where the suffixes represent the corresponding cone types; for example, $R_{L+M-/L-M+}$ in Eq. (12) represents the input to the double opponent cell which receives the excitatory signal from L on-center opponent cell after adaptation, and the inhibitory signal from L off-center opponent cell.

2.4. Opponent cells and double opponent cells

Each cell receives synaptic input and a super-threshold noisy input generated by a Poisson point process, with the mean firing rate depends on the synaptic input. The membrane potential is computed by the differential equation based on leaky integrate-and-fire model, with the same formalism and parameter values proposed by Chance et al., 1998 as follows:

$$\tau_m \frac{dV}{dt} = V_0 - V + G_E(t)(V_E - V) + G_I(t)(V_I - V), \quad (14)$$

$$V \to V_{reset} \qquad (when \quad V = V_{th})$$

where V_0 is the resting potential; V_E and V_I are the reversal potential for excitatory synapse and inhibitory synapse, respectively. When the membrane potential reaches the threshold value, the neuron fires and the membrane potential is reset. The excitatory and inhibitory synaptic conductance at time t are denoted by $G_E(t)$ and $G_I(t)$. If pre-synaptic action potential occurs, the conductance of the synapse is increased.

$$Ex: G_E \to G_E + W_E D_E S_E, \quad In: G_I \to G_I + W_I D_I S_I, \quad (15)$$

where the suffix E and I represent excitatory and inhibitory synapses, respectively. Between action potentials, both G_E and G_I decay exponentially with time constant τ_E and τ_I.

$$Ex: \tau_E \frac{dG_E}{dt} = -G_E, \quad In: \tau_I \frac{dG_I}{dt} = -G_I, \quad (16)$$

Cells receive their afferent drives via synapses that depress. The transmission efficacy at the synapse decreases, if pre-synaptic action potential occurs. The transmission efficacy recovers exponentially between action potentials. Here, fast and slow components of depression are considered in the present model. The factors D and S describe the fast and slow depressions, which occur within hundreds milliseconds and several seconds, respectively. If the synapse receives the action potential, D and S are reduced ($0 < d_j, s_j < 1$). Between pre-synaptic action potentials, D and S recover exponentially toward the value one:

$$Ex: D_j \rightarrow d_j D_j, \quad In: S_j \rightarrow s_j S_j, \tag{17}$$

$$Ex: \tau_D \frac{dD_j}{dt} = 1 - D_j, \quad In: \tau_S \frac{dS_j}{dt} = 1 - S_j, \tag{18}$$

where parameters d_j and s_j determine the amount of depression at the synapse j. τ_D, and τ_S are time constants for controlling the depression recovery rates.

2.5. Long-term synaptic plasticity

The model assumes long-term synaptic plasticity between opponent cells and double opponent cells; the strength of the connections can alter depending on the relative timing of the pre-synaptic and the post-synaptic spike. If post-synaptic spike occurs immediately after the pre-synaptic spike, the strength of the synaptic connection W increases (Eq. 19); otherwise, returns gradually to the normal value (Eq.20). The weights of excitatory synapse W_E and inhibitory synapse W_I are updated as follows:

$$W_E \rightarrow W_E + w_{j\_Elong} d_{j\_Elong}, W_I \rightarrow W_I + w_{j\_Ilong} d_{j\_Ilong}, \tag{19}$$

$$\tau_{E\_long} \frac{dW_E}{dt} = -W_E, \quad \tau_{I\_long} \frac{dW_I}{dt} = -W_I, \tag{20}$$

where w_j and the time constant τ_{long} determines in what degree the connection is strengthened by an update, and we refer to the values proposed by Izhikevich et al., 2004.

The output of the model is calculated from spike frequency of double opponent cells. We use the index in the results which expressed with the subtracted and normalized difference between the responses of M double opponent cell from that of L double opponent cell. The index corresponds to the equilibrium point between two colors.

3. Results

Figure 2 shows the temporal evolution of index in the very short-term exposure of chromatic light. The index approaches to the value before onset immediately after the exposure of chromatic flash light. Although the dynamics faster than several tens of milliseconds is mostly cased by the retinal adaptive process, the period until the color appearance reaches to steady state become longer with the consideration with adaptive modulation in the visual pathway subsequent to the retina. The temporal characteristics predicted by the present model agree with the experimental study reported by Hughes, 2003.

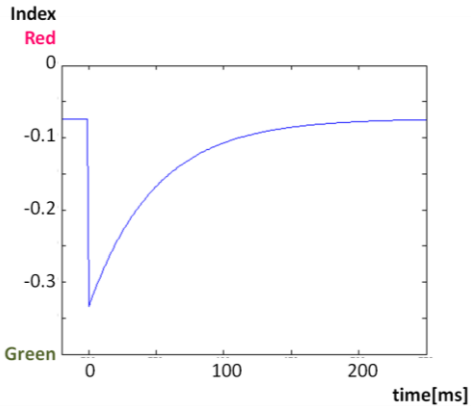

Fig.2. temporal change of the color appearance in very short-term exposure of chromatic light.

Next, we investigated the shift of the equilibrium point during very long-term adaptation. The simulation result is shown in Fig.3. In this simulation, the model received long-wavelength illumination for 8 hours per day for long-term adaptation and normal illumination (white) except adaptation hours, according to the setting of the reported study (Neitz, 2002; Belmore, 2008). The index, which corresponds to the equilibrium point or unique yellow, progressively away from the balanced point, and the changed perceptions persist for days.

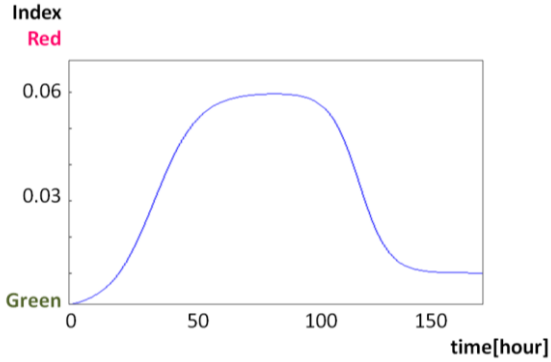

Fig.3. Shift during long-term adaptation. The model reproduces the progressive shift of the color appearance, reported by Belmore, 2008.

Fig. 4 shows the simulation result in hypothetical condition in which chromatic adaptation continues without stopping to investigate how fast the characteristics of long-term adaptation appear. Additionally, we simulated the model without long-term synaptic plasticity between opponent cell and double opponent cell i.e., long-term plasticity cannot occur, shown in broken line in Fig. 4. In the simulation without long-term plasticity, the index shifted toward the direction of adapted color, and sustained. However, the index showed only the limited return to the normal value afterwards. The result

suggested that long-term synaptic plasticity plays a key role to mediate color appearances in long-term adaptation.

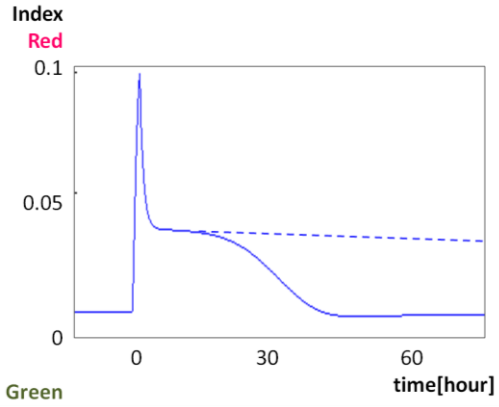

Fig.4. Shift of equilibrium point during long-term adaptation in hypothetical condition

4. Discussion

Our model reproduces the experimental results reported in the previous studies, and accounts for the change in color appearance during and after the adaptation with a broad range of temporal scales. The adaptive mechanisms at different stages in the primate visual pathway function in different temporal scales. Furthermore, the difference of time constant between excitatory synapse and inhibitory synapse cause the dynamics that equilibrium point shifts progressively toward the direction of the adapted color, and then return to the normal.

The model showed the possibility that changes in the pre-synaptic connection of double opponent cells can elicit the sustained shifts in chromatic perception. Double opponent cells respond well to chromatic edges because there is not only color opponency but also spatial opponency. These properties of double opponent cell and the pre-synapse may explain the very long-lasting aftereffect led by McCollough effect and Anti-McCollough effect in which colorless gratings appear colored depending on the orientation of the gratings.

Although the present model focuses on the temporal characteristics led by chromatic adaptation, the other phenomena such as chromatic induction are known which affects color perception. From physiological perspective, the effect of lateral connections and inputs from remote area in receptive field should be considered for more accurate prediction of color appearance.

5. Summary

We propose a computational model of the primate visual pathway, which explains the change in color appearance during and after the adaptation with a broad range of temporal scales. The model reproduces not only the fast dynamic properties of color vision, but also the shift of equilibrium yellow during and after long-term chromatic adaptation. This study suggests that multi-stage adaptation mechanism including synaptic plasticity plays a key role to fulfill stable color perception.

Acknowledgement

This research is partially supported by the Aihara Project, the FIRST program from JSPS, initiated by CSTP.

References

[1] A. Hughes and P. J. DeMarco, Jr., “Time course of adaptation to stimuli presented along cardinal lines in color space”, *J. Opt. Soc. Am. A*, vol.20, No.12, pp.2216–2227, 2003

[2] H. Momiji, A. A. Bharath, M. W. Hankins, and C. Kennard, “Numerical study of short-term afterimages and associate properties in foveal vision”, *Vis. Res.* Vol.46, pp.365–381, 2006

[3] A. Eisner and J. M. Enoch, “Some effects of I week's monocular exposure to long-wavelength stimuli,” *Perception & Psychophysics*, vol.31, pp.169-174, 1982.

[4] J. Neitz, J. Carroll, Y. Yamauchi, M. Neitz, and D. R. Williams, “Color perception is mediated by a plastic neural mechanism that is adjustable in adults.” *Neuron* vol.15, pp.783–792, 2002.

[5] S. C. Belmore, and S. K. Shevell, “Very-long-term chromatic adaptation: Test of gain theory and a new method”, *Vis. Neurosci.*, vol.25, pp.411–414, 2008.

[6] V. C. Smith and J Pokorny, “Spectral sensitivity of the foveal cone photopigments between 400 and 500 nm”, *Vis. Res.*, vol.15, 2, pp.161-171, 1975.

[7] R. Dahari and H. Spitzer, “Spatio-temporal adaptation model for retinal ganglion cells”, *J. Opt. Soc. Am. A*, vol.13, pp.419–439, 1996.

[8] H. Spitzer, and S. Semo, “Color constancy: A biological model and its application for still and video images.” *Pat. Recog.*, vol.35, pp.1645–1659, 2002.

[9] F. S. Chance, S. B. Nelson, and L. F. Abbott, “Synaptic depression and the temporal response characteristics of V1 cells”, *J. Neurosci.*, vol.18, (12) pp.4785-4799, 1998.

[10] E. M. Izhikevich, J. A. Gally and G. M. Edelman, “Spike-timing Dynamics of Neuronal Groups”, *Cerebral. CORTEX.*, Vol. 14, pp. 933–944, 2004.